pH-activated Nanoparticles for Controlled Topical Delivery of Farnesol to Disrupt Oral Biofilm Virulence

Benjamin Horev,[1,§] Marlise I. Klein,[2,‡,§], Geelsu Hwang,[3] Yong Li, [3,∞] Dongyeop Kim, [3,∞] Hyun Koo,[2,3,4,*,∞], and Danielle S.W. Benoit[1,5,6]

[1]Department of Biomedical Engineering, University of Rochester, NY 14627, United States [2]Center for Oral Biology, University of Rochester, NY 14627, United States [3]Biofilm Research Lab, Levy Center for Oral Health, University of Pennsylvania, PA 19104, United States, [4]Department of Orthodontics and Divisions of Pediatric Dentistry and Community Oral Health, School of Dental Medicine, University of Pennsylvania, PA 19104, United States, [5]Department of Chemical Engineering, University of Rochester, NY 14627, United States, [6]Center of Musculoskeletal Research, University of Rochester, NY 14627, United States, [‡]Current address: Department of Dental Materials and Prosthodontics, Araraquara Dental School, Univ Estadual Paulista, UNESP, Sao Paulo, Brazil.

* Address correspondence to: benoit@bme.rochester.edu; koohy@dental.upenn.edu

[§] Authors contributed equally to this work.

[∞]Were involved in *in vivo* efficacy testing herein.

Supplemental Figures

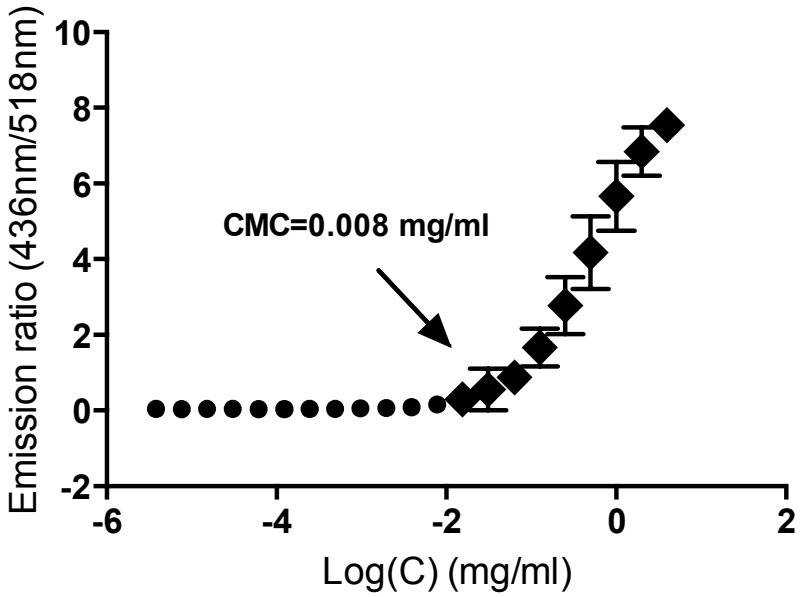

Figure S1. Critical micelle concentration (CMC) of nanoparticles. A range of nanoparticles concentrations was incubated with PRODAN® and the ratio of fluorescent emissions in hydrophobic phase/hydrophilic phases was plotted versus log(micelle concentration). CMC was determined as a concentration at which the emission ratio begins to increase with polymer concentration. The error bars represent standard error of measurements (n=3).

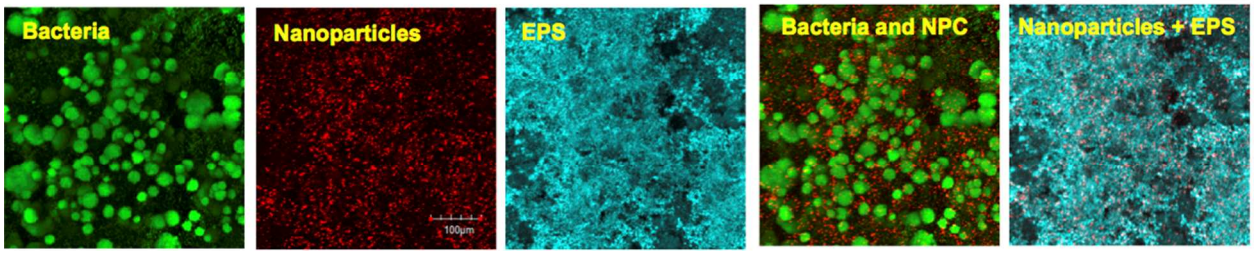

Figure S2. Confirmation of free nanoparticle attachment to *S. mutans* biofilms treated surfaces. Bacteria within biofilms forming microcolonies are depicted in green (SYTO 9 labeled), nanoparticles are depicted in red (Texas Red labeled), and EPS in blue (AlexaFluor 647 labeled).

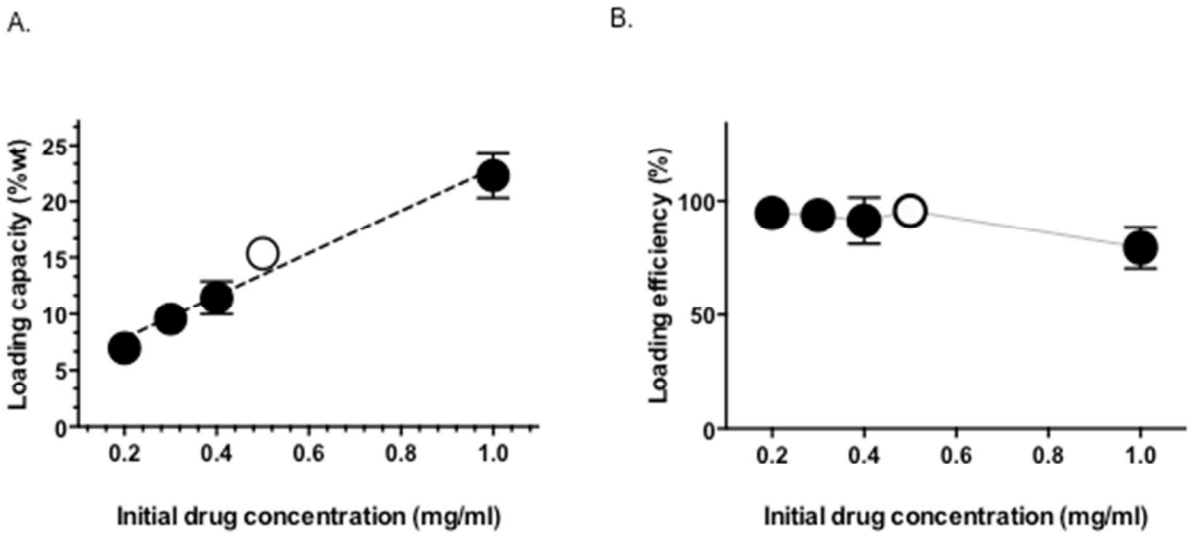

Figure S3. Nanoparticle loading at a range of drug concentrations. A. Loading capacities and **B.** loading efficiencies of nanoparticles. Blue data points denote loading capacities and efficiencies at which biofilm treatments were performed (15 wt%, 97%). Error bars represent standard error (n=3 independent experiments). As significant Pearson's correlation (dotted line, R^2>0.86) between loading capacity and initial drug concentration at loading was determined by two-tailed t-test on Pearson's correlation ($p<0.0001$). The solid line in figure S4B is a guide to an eye.

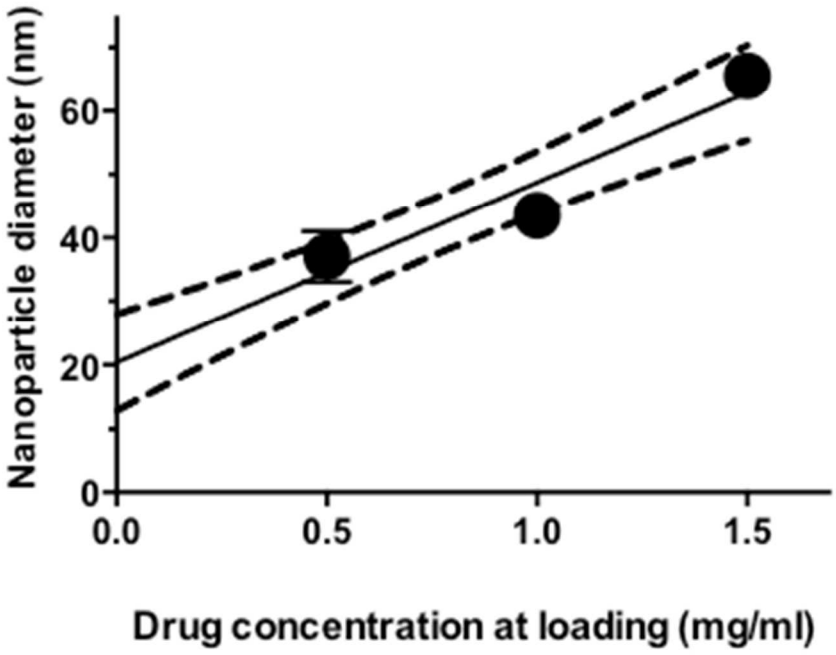

Figure S4. Increase in nanoparticle size upon loading. Nanoparticle sizes were examined by dynamic light scattering (DLS) upon loading at a range of drug concentrations (0-1.5 mg/ml). Error bars represent standard error of measurement (n=2).

A.

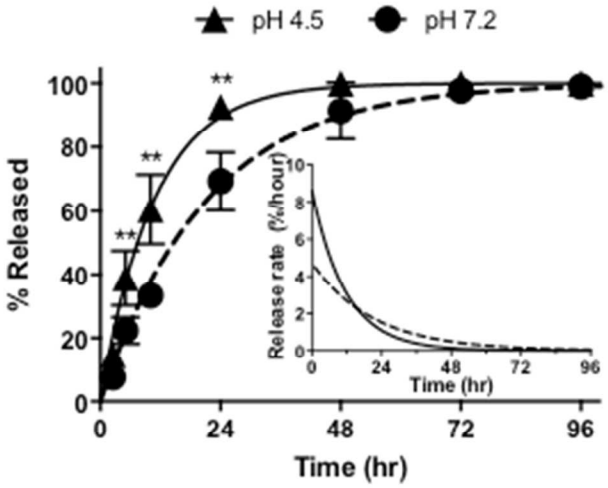

B.

pH	k_{obs} (1/hr)	$t_{1/2}$ (h)	r_0 (MIC/h)
4.5	0.26	2.7	~11
7.2	0.12	5.8	~5

Figure S5. pH-responsive release of farnesol-loaded nanoparticles in adsorption buffer. A. Farnesol release profiles at pH 7.2 and 4.5, including farnesol release rates (inset). Solid and dotted lines show fits (R^2>0.98) to first-order drug release and release rates determined by first derivative of the fits (inset). **B.** Kinetic parameters of release determined from fits to first order release (R^2>0.98). Initial release rate (A. inset, r_0), release rate constant (k_{obs}) and half-time of release ($t_{1/2}$) at pH 4.5 suggest 2-fold faster release at pH 4.5 as compared to pH pH 7.2, similar to data reported for PBS release experiments (Figure 3). Asterisks denote significant differences at p<0.01, as determined by two-way ANOVA followed by Tukey's test for multiple comparisons. Adsorption buffer composition: 50 mM KCl, 1.0 mM KPO_4, 1.0 mM $CaCl_2$, 0.1 mM $MgCl_2$, pH 6.5.

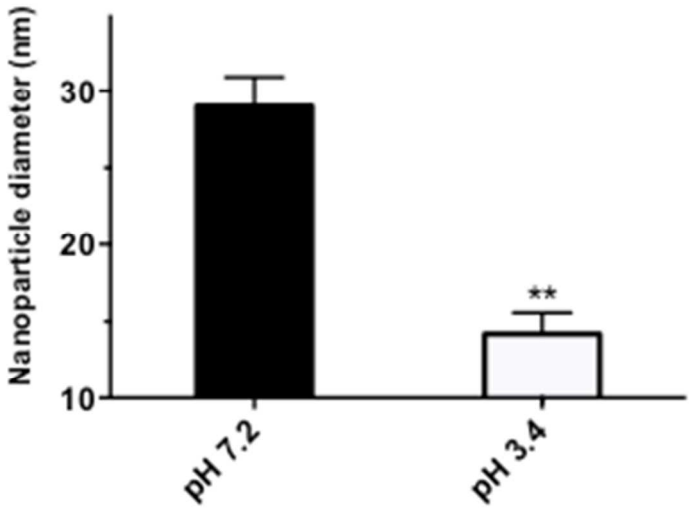

Figure S6. pH-responsive mechanism of nanoparticle structure destabilization. Nanoparticles demonstrate the pH-responsive structure destabilization at acidic pH. As a result of exposure to extreme acidic pH, ~2-fold decrease in nanoparticle diameter was observed due to

protonation and repulsion of DMAEMA residues within nanoparticle coronas and cores. Error bars represent SEM (n=5) and the asterisks denote as significant difference ($p<0.001$).

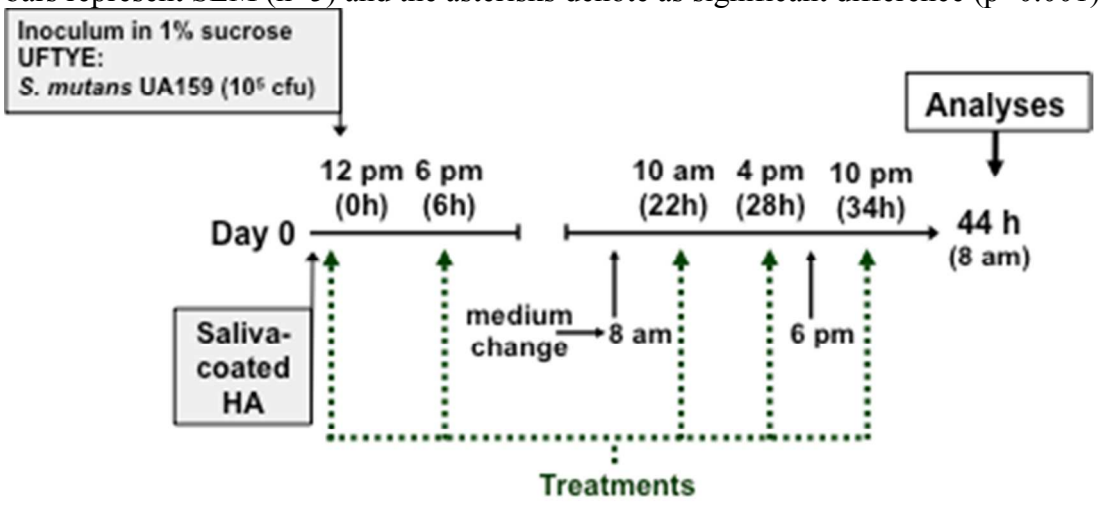

Figure S7. Treatment regimen during biofilm prevention assay. Biofilms were formed on sHA surfaces, and treated with either farnesol-loaded nanoparticles (15 wt%) or controls using clinically-relevant treatment regimen of 2-3 treatments per day.